The Build-Up of Aerosols Carrying the SARS-CoV-2 Coronavirus, in Poorly Ventilated, Confined Spaces
Supplementary Material

Björn Birnir*
Center for Complex and Nonlinear Science
Department of Mathematics
University of California, Santa Barbara
Santa Barbara, CA 93106
and
Luiza Angheluta
The Njord Centre, Department of Physics
University of Oslo, P. O. Box 1048, 0316 Oslo, Norway

November 2020

A Lagrangian Turbulence and Structure Functions

The difference between the Eulerian and the Lagrangian description of fluid flow is the frame of reference of the observer (measurements) of the flow. In the Eulerian description the observer is stationary and the fluid flows by him or her. In the Lagrangian frame of reference the observer travels with the flow and make his or her measurements in this traveling frame of reference. The mathematical description in the Eulerian frame is the conventional Navier-Stokes equation, but in the Lagrangian frame it is the Navier-Stokes equation with the material derivative $\frac{Du}{DT} = \frac{\partial u}{\partial t} + u \cdot \nabla u$ where the time variable T is the Lagrangian time, u is the fluid velocity and t the Eulerian time. The Lagrangian description is natural for the droplet/aerosols transmission, since the natural frame of reference is the one traveling with the droplet/aerosol, to see where it originates and where it ends up.

The Eulerian description is the traditional description of homogeneous turbulence, see [4, 9], and boundary turbulence, see [15, 7]. When particles or fluid droplets, such as the droplet/aerosols carrying the coronavirus, are entrained in the (air) flow, the Lagrangian description is more appropriate. We want to travel with (in the frame of reference of) the turbulent cloud and see how the droplet/aerosols interact with the cloud and each other. We want to determine if and where the

*and the University of Iceland, School of Natural Sciences, 107 Reykjavík, Iceland

droplet/aerosols settle on the ground or on surfaces, or if they remain airborn. In the latter case, we want to determine to what destinations they are carried by the turbulent flow of air. The strength of the turbulence in the flow is given by the dimensionless Reynolds number $Re = \frac{uL}{\nu}$, where L is a typical spacial dimension of the flow and ν is the kinematic viscosity. In practice, one uses the Taylor-Reynolds number $Re_\lambda = \frac{u\lambda}{\nu}$, where λ is the correlation length in the flow. We will use the approximation $Re_\lambda \approx \sqrt{10Re}$.

To compute the Richardson probability density function (PDF), see Appendix B, for the droplet/aerosols that are passive scalars, we must construct the Lagrangian velocity structure functions (LVSF) [14, 1],

$$S_p(\tau) = \langle |u(T+\tau) - u(T)|^p \rangle = \langle |\delta u|^p \rangle,$$

for $p = 2$, where τ is a temporal lag-variable measuring the time passed between two observations of the flow, and $\langle \cdot \rangle$ is an ensamble average over many measurements.

The Kolmogorov-Obukhov theory determines the scaling laws in Lagrangian turbulence, for small τ,

$$S_p \sim \tilde{C}_p (\varepsilon\tau)^{p/2},$$

see [12, 11], where ε is the dissipation rate in the flow, and $\tilde{C}_p$ are constants, that are not universal, but depend on the configuration of the flow. In particular, for $p = 2$, we get $S_2 \sim \tilde{C}_2 \varepsilon\tau$, see [14]. Although the Lagrangian turbulent flow follows these scaling laws for τ sufficiently small, it quickly deviates from the predicted scaling exponents and approaches values of the scaling exponents that are more similar to their values in Eulerian turbulence [14]. In between, there is a "passover" interval where the values of the exponents dip significantly below either their initial or eventual values, see [14].

In [1], the authors adapt the methods developed in [7], for boundary layer turbulence, to compute all the Lagrangian velocity structure functions. In [7] they had encountered a similar "passover region". This was the buffer region separating the viscous from the inertial layer in pipe and boundary turbulence. The authors were able to overcome this obstacle by adapting a "spectral function" introduced in [8] to compute the mean velocity in boundary and pipe flow, and generalize it to also model the buffer layer. This explains the shape of the scaling exponents observed in simulations and experiments [14]. We use these results, for $S_2 = \langle |\delta u|^2 \rangle$ in Lagrangian turbulence, see Figure 8, applied to the restaurant, see Figure 7.

B The Richardson Scaling

Diffusion of droplets or particles was modeled by Richardson [13] who assumed that the diffusivity is,

$$D_R = \frac{d\langle r^2 \rangle}{dt} = k_0 \varepsilon^{1/3} \langle r^2 \rangle^{2/3},$$

based on empirical evidence where $r(t)$ is the particle separation at time t. The solution of this equation gives

$$\langle r^2(t) \rangle = g\, \varepsilon\, t^3,$$

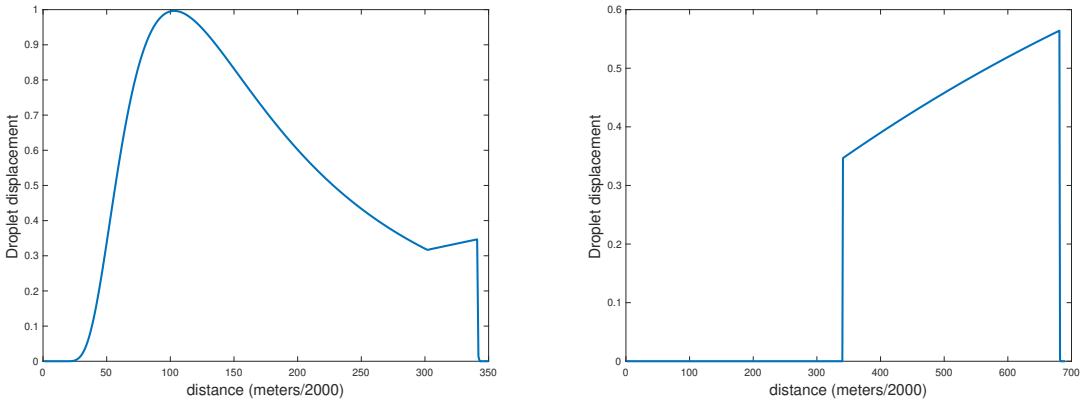

Figure 1: The initially exhaled (left) and subsequently propagated (right) spatial distributions of droplet displacement.

where $g = k_0^3/27$ is called the Richardson constant. This is know as Richardson diffusion. Obukhov [12] gave a derivations based on the Kolmogorov-Obukhov scaling

$$D_R = \frac{d\langle r^2\rangle}{dt} = \tau(r)\langle(\delta u)^2\rangle,$$

where δu is the Lagrangian velocity difference, so $\langle(\delta u)^2\rangle$ is the second Lagrangian structure function and $\tau(r)$ is the eddy turnover time. Now according to the Kolmogorov-Obukhov Theory, $\langle(\delta u)^2\rangle = C_2\varepsilon^{2/3}r^{2/3}$ and $\tau(r) = \varepsilon^{-1/3}r^{2/3}$, so

$$\frac{d\langle r^2\rangle}{dt} = \tau(r)\langle(\delta u)^2\rangle = C_2\varepsilon^{1/3}r^{4/3}.$$

The solution is

$$\langle r^2(t)\rangle = \frac{C_2}{27}\varepsilon\, t^3,$$

or $g = \frac{C_2}{27}$. This holds for $\eta << r_0 < \langle r^2(t)\rangle^{1/2} << L$, where η is the Kolmogorov constant and L is the system size. r_o is the initial particle separation.

In addition to this region, there is a ballistic regime derived by Batchelor [3]. In this regime the particles separate linearly in t depending on the initial velocity. For the initial separation of the particles r_0 very small, first there is a ballistic region and at a later time the particles separate exponentially. This marks the beginning of the Richardson diffusion.

We assume that the droplet/aerosols are passive scalar, or that they are simply carried along by the flow without influencing the flow itself. The probability density function, for the separation r of the passive scalars, satisfies the partial differential equations (PDE)

$$\partial_t P(r,t) = r^{-2}\partial_r r^2 C_{||}(r)\partial_r P,$$

where $C_{||}$ is the longitudinal correlation function. With $C_{||} \sim Dr^{4/3}$ and $P_0(r,t_0) = \delta(t-t_0)$, the PDE has an explicit solution in the large time limit, see [10] and [2],

$$P_{Ric}(r,t) \approx \frac{r^2}{\langle r^2(t)\rangle^{3/2}} \exp\left(-d(\frac{r}{\langle r^2(t)\rangle^{1/2}})^{2/3}\right),$$

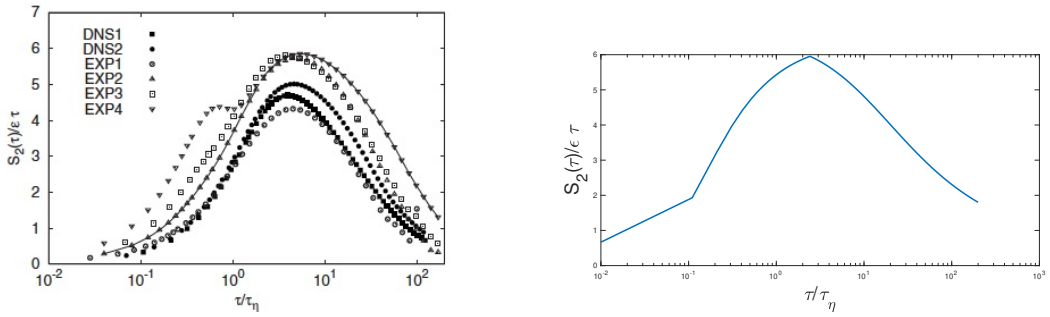

Figure 2: The experimental and simulated compensated second structure function $S_2/(\varepsilon\tau_\eta)$, from [5], (left) and the theoretical model of $S_2/(\varepsilon\tau_\eta)$ (right).

where d is a constant determined by D. This assumes that the velocity field is stochastic, incompressible, homogeneous and isotropic and δ correlated in time.

The Richardson scaling allows us to express the Richardson probability density function (PDF) in terms of the structure functions. Namely, using the above to set $r^2 = \frac{C_2}{27}\varepsilon t^3$, we get that $\tilde{C}_2 = C_2^{4/3}/3$, and

$$\langle(\delta u)^2\rangle = C_2\varepsilon^{2/3}r^{2/3} = \frac{C_2^{4/3}}{3}\varepsilon t,$$

so

$$\langle r^2(t)\rangle = \frac{1}{C_2^3\varepsilon^2}\langle(\delta u)^2\rangle^3.$$

A substitution into the PDF above gives

$$P_{Ric}(r,t) \approx \frac{C_2^{9/2}\varepsilon^3 r^2}{\langle(\delta u)^2\rangle^{9/2}}\exp\left(-\frac{9}{4}\frac{\varepsilon^{2/3}C_2 r^{2/3}}{D\langle(\delta u)^2\rangle}\right), \tag{B.1}$$

using the value $d = \frac{9}{4D}$ from [2]. D is the coefficient in the Richardson law

$$r^{2/3} = \frac{2}{3}Dt = \frac{C_2^{1/3}}{3}\varepsilon^{1/3}t,$$

so $D = \frac{1}{2}\varepsilon^{1/3}C_2^{1/3}$.

In Figure 8, we compare the compensated second structure function $S_2/(\varepsilon\tau_\eta)$, from experiments and simulations, from [5], with the theoretical model of $S_2/(\varepsilon\tau_\eta)$ used in this paper.

C Computation of the Richardson Coefficient

The second Lagrangian structure function is

$$\begin{aligned} S_2(r,t) &= \frac{4}{C^2}\sum_{k\in\mathbb{Z}\setminus 0}\left[\frac{\frac{C}{2}c_k(1-e^{-2\lambda_k t})}{|k|^{2/3}+\frac{4\pi^2\nu}{C}|k|^{2/3+\frac{4}{3}}}+\frac{|d_k|^2(1-e^{-\lambda_k t})}{|k|^{2/3}+\frac{8\pi^2\nu}{C}|k|^{2/3+\frac{4}{3}}+\frac{16\pi^4\nu^2}{C^2}|k|^{2/3+\frac{8}{3}}}\right] \\ &\quad\times(|\sin^2(\pi k\cdot r)|), \end{aligned}$$

RH	21%	35%	51%	65%	81%
k_d	0.0031	0.0078	0.016	0.024	0.028

Table 1: The viral decay coefficient $k_d = 1/time_d$ for five values of relative humidity (Influenza A), from [16] Table 3.

by the stochastic closure theory, see [6]. At $t = \infty$ and for r small we get

$$S_2(r,\infty) = \frac{4\pi^{2/3}}{C^2} \sum_{k\in\mathbb{Z}\setminus 0} \left[\frac{\frac{C}{2}c_k}{1+\frac{4\pi^2\nu}{C}|k|^{\frac{4}{3}}} + \frac{|d_k|^2}{1+\frac{8\pi^2\nu}{C}|k|^{\frac{4}{3}}+\frac{16\pi^4\nu^2}{C^2}|k|^{\frac{8}{3}}} \right] r^{2/3}$$

$$= \frac{4\pi^{2/3}}{C^2} \sum_{k\in\mathbb{Z}\setminus 0} \left[\frac{\frac{C}{2}b^2}{(b^2+|k|^m)^2} \frac{1}{(1+\frac{4\pi^2\nu}{C}|k|^{\frac{4}{3}})} + \frac{a^2}{(a^2+|k|^m)^2} \frac{1}{(1+\frac{8\pi^2\nu}{C}|k|^{\frac{4}{3}}+\frac{16\pi^4\nu^2}{C^2}|k|^{\frac{8}{3}})} \right] r^{2/3},$$

where we have used the models $c_k = \frac{b^2}{(b^2+|k|^m)^2}$ and $d_k = \frac{a^2}{(a^2+|k|^m)^2}$ from [9], for the coefficients c_k and d_k.

The Taylor-Reynolds number for the restaurant in Guangzhou is $Re_\lambda = 705$, the distance from the infected person to the wall with the air-conditioner is 3 meters, the air velocity in that direction is 0.25 m/s. The parameters C, a, b and m depend on the Reynolds number, we interpolate them from the values computed in [9], to get $C = 5.574$, $a = 6.508$, $b = 0.076$ and $m = 1.000$. The value of $\varepsilon = 1.2$ is obtained from [5] at $Re_\lambda = 690$, this is close to our value of 705. With this information we can compute the coefficient C_2 in the structure function $S_2(r) = C_2(705)r^{2/3}$, namely

$$\begin{aligned} C_2 &= \frac{4\pi^{2/3}}{5.574^2} \sum_{k\in\mathbb{Z}\setminus 0} \left[\frac{2.787\times 0.076^2}{(0.076^2+|k|)^2} \frac{1}{(1+\frac{4\pi^2\nu}{5.574}|k|^{\frac{4}{3}})} + \frac{6.508^2}{(6.508^2+|k|)^2} \frac{1}{(1+\frac{8\pi^2\nu}{5.574}|k|^{\frac{4}{3}}+\frac{16\pi^4\nu^2}{5.574^2}|k|^{\frac{8}{3}})} \right] \\ &= 0.489. \end{aligned}$$

This gives the exponent in the Richardson PDF,

$$d = \frac{9}{4D} = \frac{9}{2C_2^{1/3}\varepsilon^{1/3}} = 5.376.$$

D The Aerosol Concentration

The life-time of the SARS-CoV-2 Coronavirus in aerosols is affected by relative humidity (RH) but the exact relationship is not known yet. The dependance is presumed to be similar to that of Influenza A and we use the values for Influenza A, from [16] Table 3, as a proxy. The RH values and the corresponding values of k_d are given in Table 1.

In Figure 9, we show the aerosols concentrations as a function of time corresponding to the values in Table 1. The first two value of RH (left figure) give concentrations bounded below by a quadratic polynomial, the last three (right figure) give concentrations bounded below by a quintic polynomial. In all of these cases the aerosol concentration is rapidly increasing over the span of one hour.

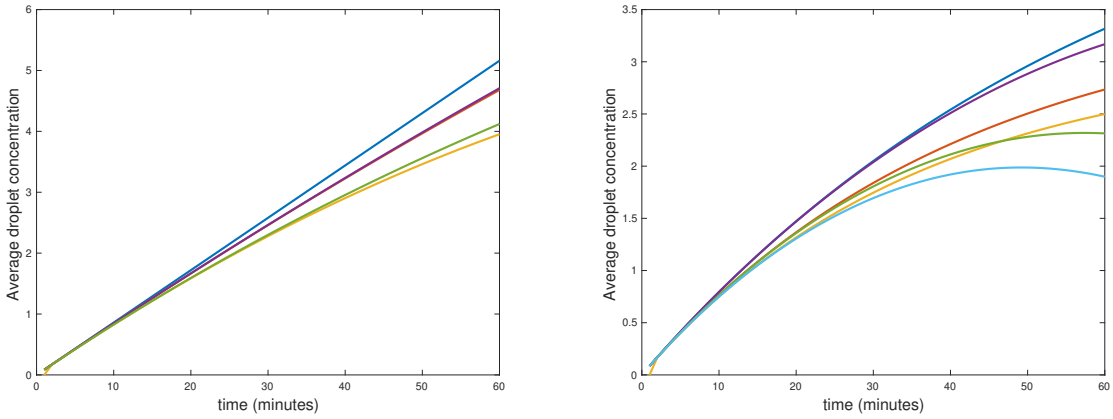

Figure 3: (Left) The aerosol concentration for *one hour*, top (blue) solution of the ODE, RH 21%, bounded below by a quadratic polynomial (scarlet), bottom (green) solution of the ODE, RH 35%, bounded below by a quadratic polynomial (yellow). (Right) The aerosol concentration for *one hour*, top (blue) solution of the ODE, RH 51%, bounded below by a quintic polynomial (scarlet), middle (red) solution of the ODE, RH 65%, bounded below by a quintic polynomial (green), bottom (yellow) solution of the ODE, RH 81%, bounded below by a quintic polynomial (light blue).

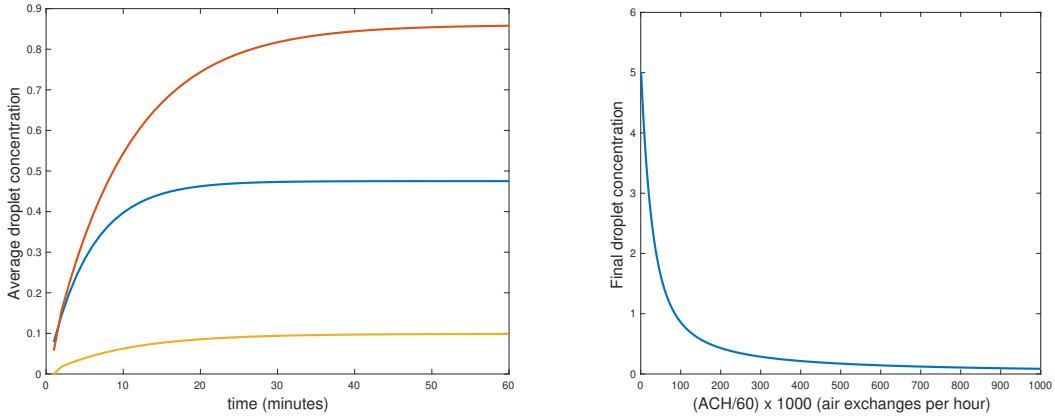

Figure 4: (Left) The aerosol concentration, for *one hour* with ventilation, solutions of the ODE, top (red) 6 ACH , middle (blue) 10 ACH (8 l/s per person), bottom (yellow) the ventilation that works 52 ACH. (Right) The aerosol concentration after *one hour* as a function of ventilation. The leftmost point corresponds to 60 ACH.

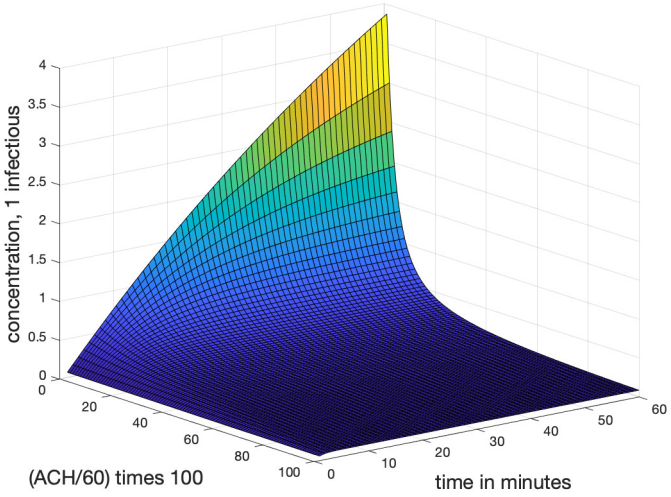

Figure 5: (Left) The aerosol concentration as a function of time and ventilation. The peak corresponds to poor ventilation, the low edge of the plateau to a safe (52 ACH) ventilation.

In Figure 10, we show the effect of ventilation. Because of the density of people in the restaurant, it is difficult to ventilate. A strong ventilation 6 ACH only reduces the concentration to 0.86 in one hour, a value that is still highly contagious. Basing the ventilation on the number of people in the contaminated part of the restaurant, 8 liters per second per person, does a little better but still leaves the concentration at almost 0.5 after one hour. This was the improvement in ventilation that we discussed in the Discussion Section above. Increasing the ventilation to 52 ACH finally brings the concentration down below the acceptable level 0.1, see the left hand side of Figure 10. On the right hand side of Figure 10 we show the aerosol concentration after one hour as a function of increasing ventilation. This figure makes it clear the restaurant is difficult to ventilate and requires 60 ACH before the contamination is mostly eliminated.

In Figure 11, we show the aerosol concentration as function of ventilation and time. It is clear that with little or no ventilation the concentration quickly builds up to very contagious levels but is brought sharply down by increasing the ventilation. However, to bring it to safe levels requires a very strong ventilation.

We have used used the Lagrangian computation to find the parameters in the ODE **??**. But this was only to find the volume of the contaminated pyramid, see Figure **??**. Once the Lagrangian cloud is found much more can be done. In particular, with ventilation, a configuration of restaurant tables can be found that makes next neighbor infection unlikely. In principle, we can even simulate how the aerosol cloud enters the ventilation system and is spread by, it on the average.

References

[1] ANGHELUTA, L., AND BIRNIR, B. The velocity structure functions in Lagrangian turbulence. *To appear* (2020).

[2] BALKOVSKY, E., AND LEBEDEV, V. Instanton for the kraichnan passive scalar problem. *Physical Review E 58*, 5 (1998), 5776.

[3] BATCHELOR, G. K. *The Theory of Homogenous Turbulence*. Cambridge Univ. Press, New York, 1953.

[4] BATCHELOR, G. K. *Homogeneous Turbulence*. Cambridge University Press, 1960.

[5] BIFERALE, L., BODENSCHATZ, E., CENCINI, M., LANOTTE, A. S., OUELLETTE, N. T., TOSCHI, F., AND XU, H. Lagrangian structure functions in turbulence: A quantitative comparison between experiment and direct numerical simulation. *Physics of Fluids 20*, 6 (2008), 065103.

[6] BIRNIR, B. The Kolmogorov-Obukhov statistical theory of turbulence. *J. Nonlinear Sci.* (2013). DOI 10.1007/s00332-012-9164-z.

[7] BIRNIR, B., ANGHELUTA, L., KAMINSKY, J., AND CHEN, X. Spectral link of the Generalized Townsend-Perry constants in turbulent boundary layers. *Physical Review Research Submitted* (2020).

[8] GIOIA, G., GUTTENBERG, N., GOLDENFELD, N., AND CHAKRABORTY, P. Spectral theory of the turbulent mean-velocity profile. *Physical Review Letters 105* (2010).

[9] KAMINSKY, J., BIRNIR, B., BEWLEY, G., AND SINHUBER, M. Reynolds number dependence of the structure functions in homogeneous turbulence. *Journ. of Nonlin. Sci.* (2020), 1–34.

[10] KRAICHNAN, R. H. Lagrangian-history closure approximation for turbulence. *Phys. Fluids 8* (1965), 575–598.

[11] MONIN, A., AND YAGLOM, A. Mechanics of turbulence. *Statistical fluid mechanics 2* (1975).

[12] OBUKHOV, A. Spectral energy distribution in a turbulent flow. *Izv. Akad. Nauk. SSSR. Ser. Geogr. i. Geofiz 5* (1941), 453–466.

[13] RICHARDSON, L. F. Atmospheric diffusion shown on a distance-neighbour graph. *Proceedings of the Royal Society of London. Series A, Containing Papers of a Mathematical and Physical Character 110*, 756 (1926), 709–737.

[14] TOSCHI, F., AND BODENSCHATZ, E. Lagrangian properties of particles in turbulence. *Annual review of fluid mechanics 41* (2009), 375–404.

[15] TOWNSEND, A. A. *The Structure of Turbulent Shear Flow*. Cambridge University Press, 1976.

[16] YANG, W., AND MARR, L. C. Dynamics of airborne influenza a viruses indoors and dependence on humidity. *PloS one 6*, 6 (2011), e21481.